

PAPER

# Determination of the band offsets of the $\text{Ga}_2\text{O}_3$ :Si/FTO heterojunction for current spreading applications

To cite this article: Carlos G Torres-Castanedo *et al* 2020 *J. Phys. D: Appl. Phys.* **53** 314003

View the [article online](#) for updates and enhancements.



**IOP | ebooks™**

Bringing together innovative digital publishing with leading authors from the global scientific community.

Start exploring the collection—download the first chapter of every title for free.

# Determination of the band offsets of the Ga<sub>2</sub>O<sub>3</sub>:Si/FTO heterojunction for current spreading applications

Carlos G Torres-Castanedo<sup>1</sup> , Kuang-Hui Li<sup>1</sup>, Laurentiu Braic<sup>2</sup> and Xiaohang Li<sup>1,3</sup> 

<sup>1</sup> King Abdullah University of Science and Technology (KAUST), Advanced Semiconductor Laboratory, Thuwal 23955-6900, Saudi Arabia

<sup>2</sup> King Abdullah University of Science and Technology (KAUST), Core Labs, Thuwal 23955-6900, Saudi Arabia

E-mail: [xiaohang.li@kaust.edu.sa](mailto:xiaohang.li@kaust.edu.sa)

Received 28 January 2020, revised 29 March 2020

Accepted for publication 31 March 2020

Published 29 May 2020



## Abstract

Because of the relatively low electron mobility of Ga<sub>2</sub>O<sub>3</sub>, it is important to identify suitable current spreading materials. Fluorine-doped SnO<sub>2</sub> (FTO) offers superior properties to those of indium tin oxide (ITO), including higher thermal stability, a larger bandgap, and lower cost. However, the Ga<sub>2</sub>O<sub>3</sub>:Si/FTO heterojunction, including the important band offsets and the *I*–*V* characteristics, have not previously been reported. In this work, we have grown a Ga<sub>2</sub>O<sub>3</sub>:Si/FTO heterojunction and performed x-ray photoelectron spectroscopy measurements. The conduction and valence band offsets were determined to be 0.11 and 0.42 eV, indicating a minor barrier for electron transport and a type-I heterojunction. The subsequent *I*–*V* measurement of the Ga<sub>2</sub>O<sub>3</sub>:Si/FTO heterojunction exhibited pseudo-ohmic behavior. The results of this work support the potential of FTO for the current spreading layers of Ga<sub>2</sub>O<sub>3</sub> devices for high temperature and ultraviolet applications.

Keywords: gallium oxide, FTO, band offset, current spreading layer

(Some figures may appear in colour only in the online journal)

The ultrawide-bandgap semiconductor gallium oxide (Ga<sub>2</sub>O<sub>3</sub>) has the potential for use in superior power and optical devices. Different devices using Ga<sub>2</sub>O<sub>3</sub> have been demonstrated such as MOSFETs [1], MESFETs [2], FinFETs [3], and solar-blind ultraviolet photodetectors (SBDs) [4]. Recently, Green *et al* [5] reported a Ga<sub>2</sub>O<sub>3</sub>-based MOSFET with a critical electric field of 3.8 MV cm<sup>−1</sup>, the highest value reported for any transistor. This value is close to half of the theoretical value for Ga<sub>2</sub>O<sub>3</sub> (8 MV cm<sup>−1</sup>) but is already higher than the theoretical limits for GaN (3 MV cm<sup>−1</sup>) and SiC (3.2 MV cm<sup>−1</sup>) [6]. Ga<sub>2</sub>O<sub>3</sub> is also suitable for SBDs due to its large bandgap (4.7–4.9 eV) [7–9] and for gas sensors due to its thermal and chemical stability [10]. For example, Ga<sub>2</sub>O<sub>3</sub> thin films have been employed as O<sub>2</sub> sensors at high operating temperatures up to 1000 °C [11]. Moreover, the availability of conductive Ga<sub>2</sub>O<sub>3</sub>

substrates makes this material suitable for vertical injection in visible and ultraviolet (UV) III-nitride LED technology [12–14].

Ohmic contacts with low contact resistance are essential to accelerate the development of Ga<sub>2</sub>O<sub>3</sub>-based devices. Good p-type doping has not been realized for Ga<sub>2</sub>O<sub>3</sub> [15, 16] and thus the discussion of the ohmic contact and the current spreading layer refers to n-type Ga<sub>2</sub>O<sub>3</sub> only. Recently, the ohmic behavior of nine different metals on n-type Ga<sub>2</sub>O<sub>3</sub> has been studied, showing that In/Au and Ti/Au form ohmic contact after annealing at 600 °C and 400 °C–500 °C, respectively [17, 18]. However, the ohmic contacts are not sufficient for high performance Ga<sub>2</sub>O<sub>3</sub> devices. Because of the relatively low electron mobility of Ga<sub>2</sub>O<sub>3</sub> (up to 8.2 S cm<sup>−1</sup>) [19], it is crucial to develop a current spreading layer to reduce current crowding and contact resistance. Recently, Sn-doped indium oxide (ITO) has been studied as a current spreading layer to improve the ohmic contact between metal and Ga<sub>2</sub>O<sub>3</sub> [20].

<sup>3</sup> Author to whom any correspondence should be addressed.

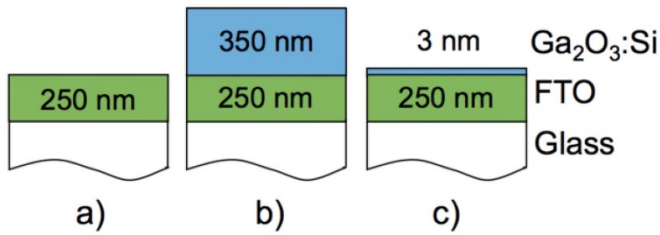


**Figure 1.** Schematics of the three investigated samples: (a) the commercial FTO/glass substrate, and (b) the thick (350 nm) and (c) the thin (3 nm)  $\text{Ga}_2\text{O}_3\text{:Si}$  layers deposited on the FTO/glass substrates.

The conduction and valence band offsets (CBO and VBO) of the  $\text{Ga}_2\text{O}_3\text{/ITO}$  were recently determined to be 0.32 and 0.78 eV, respectively, by Carey *et al* [21]. However, ITO is not an ideal candidate for high temperature and UV applications, as it is thermally unstable at high processing or device operation temperatures [22–24]. Also, the bandgap of ITO is around 4 eV, which makes it absorptive for optical applications below 350 nm. On the other hand, fluorine-doped  $\text{SnO}_2$  (FTO) could be a better candidate since it is thermally stable even at temperatures higher than 600 °C [25]. This excellent thermal stability is, in particular, important for  $\text{Ga}_2\text{O}_3$ -based devices as their thermal conductivity is poor which may cause self-heating effects [26]. Moreover, the bandgap of FTO is moderately larger than that of ITO, as measured in this study and presented below, thus covering a wider range of spectrum in terms of optical transparency. Furthermore, it is worth mentioning that FTO has a lower cost than ITO due to the scarcity of indium, which can lower the overall device cost [27].

To explore the potential of FTO as a current spreading layer for n-type  $\text{Ga}_2\text{O}_3$ , it is essential to identify the band alignment of the  $\text{Ga}_2\text{O}_3\text{/FTO}$  heterojunction. Ideally, there is no considerable potential barrier for electron transport at the conduction band edge. Furthermore, a non-rectifying electrical behavior would allow FTO to be employed to complement or replace metal contacts, or serve as the current spreading layer. In this study, we report on the band offset measurement of n-type  $\text{Ga}_2\text{O}_3$  grown on commercial FTO substrates using x-ray photoelectron spectroscopy (XPS). The crystal structure and optical transmission of the films were studied using x-ray diffraction (XRD) and UV–Vis spectroscopy. The binding energies and core levels of Ga  $2p_{3/2}$  and Sn  $3d_{5/2}$  were investigated. The VBO and CBO are determined, where a type-I junction was found. Finally, the Ti/Au metal pads were deposited and annealed to measure the  $I$ – $V$  curve of the  $\text{Ga}_2\text{O}_3\text{:Si/FTO}$  heterojunction. The study paves the way for the use of FTO as the current spreading layer for high temperature and UV applications based on  $\text{Ga}_2\text{O}_3$ .

$\text{Ga}_2\text{O}_3$  thin films have been grown by different techniques such as metal–organic chemical vapor deposition [2, 28], molecular beam epitaxy [29], hydride vapor phase epitaxy [30], and pulsed laser deposition (PLD) [31] on both native and foreign substrates. The PLD technique, with its relatively low cost and high versatility, has been employed extensively in the  $\text{Ga}_2\text{O}_3$  research community [18, 32, 33]. In this study, three samples were prepared (figure 1), including a commercial

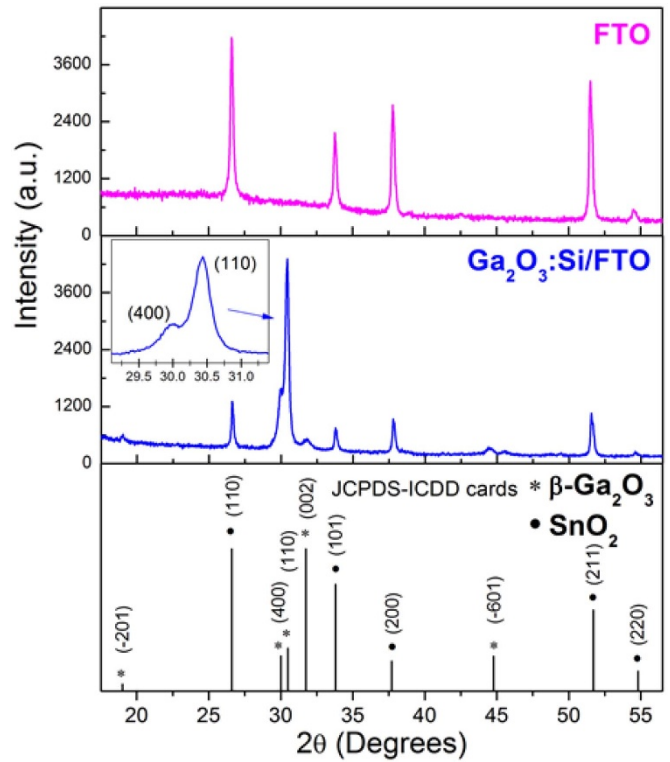


**Figure 2.** XRD patterns of the FTO/glass substrate and the 350 nm  $\text{Ga}_2\text{O}_3\text{:Si}$  film deposited on the FTO/glass substrate. The inset shows the two preferred monoclinic directions for  $\text{Ga}_2\text{O}_3\text{:Si}$  film, (110) and (400). The patterns are compared to JCPDS-ICDD cards 41-1445 ( $\text{SnO}_2$ ) and 43-1012 ( $\text{Ga}_2\text{O}_3$ ).

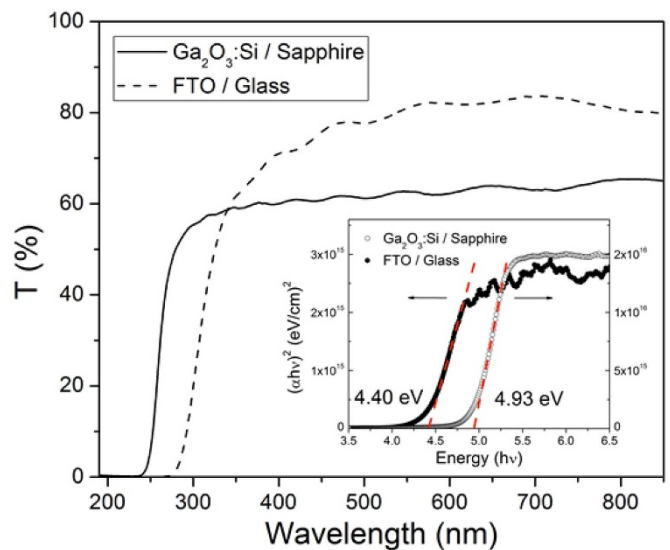


**Figure 3.** Transmission spectra of the 350 nm thick  $\text{Ga}_2\text{O}_3\text{:Si}$  thin films deposited on sapphire and FTO/glass substrates. The inset shows the Tauc plot  $h\nu$  versus  $(\alpha h\nu)^2$  with the  $E_g$  values for each film.

250 nm thick FTO thin film on a glass substrate with a sheet resistance of 6  $\Omega/\text{square}$  (NANOCS FT15-120-20), and  $\sim 350$  and  $\sim 3$  nm thick  $\text{Ga}_2\text{O}_3\text{:Si}$  thin films deposited using PLD on two FTO/glass substrates. The number of pulses used for the two depositions was 30 000 pulses and 200 pulses for the 350

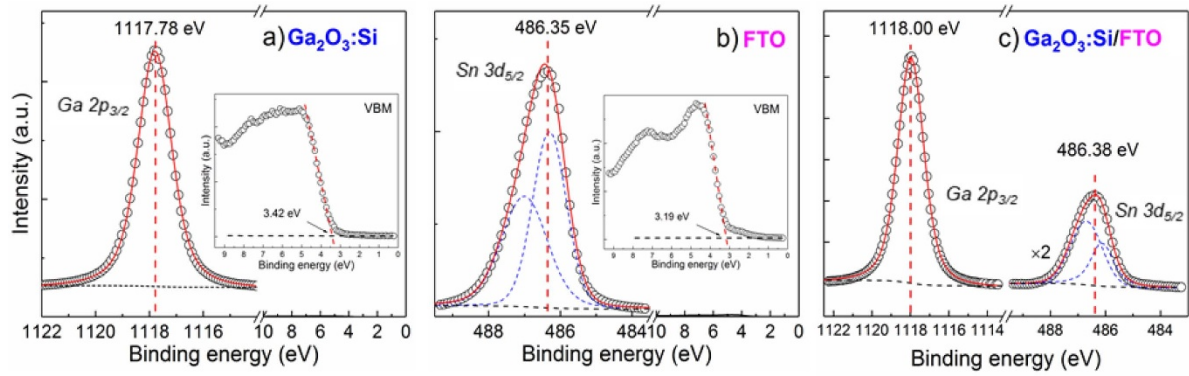


**Figure 4.** Core level Ga  $2p_{3/2}$  and VBM spectra of the  $\sim 350$  nm  $\text{Ga}_2\text{O}_3\text{:Si}$  on FTO (a). Core level Sn  $3d_{5/2}$  and VBM spectra of the 250 nm FTO (b). Core level Ga  $2p_{3/2}$  and Sn  $3d_{5/2}$  of the 3 nm  $\text{Ga}_2\text{O}_3\text{:Si}$  on FTO (c). The core levels were fitted by Voigt curves and using the Shirley background.

and 3 nm thick  $\text{Ga}_2\text{O}_3\text{:Si}$  thin films, respectively. The thicknesses were determined using the growth rate of  $0.17 \text{ \AA/pulse}$  and the number of pulses in the PLD processes. Prior to PLD, the FTO/glass substrates were sequentially cleaned ultrasonically in acetone and isopropanol, and subsequently rinsed in distilled water. Then the 350 and 3 nm  $\text{Ga}_2\text{O}_3\text{:Si}$  thin films were deposited under the same conditions using a Neocera Pioneer 180 PLD system with a chamber base pressure of less than  $1 \times 10^{-7}$  Torr, equipped with a Coherent 205F laser working at 248 nm. A one-inch  $\text{Ga}_2\text{O}_3$  target (PVD Products) with 1.6 at% Si was ablated at a repetition rate of 5 Hz and a pulse energy density of  $2 \text{ J cm}^{-2}$ . The distance between the target and the substrate was 10 cm. The  $\text{O}_2$  pressure was 4.5 mTorr and the substrate temperature was  $575^\circ\text{C}$ . This temperature is higher than the ITO stability temperature [24–26] which enables high temperature deposition of crystallized  $\text{Ga}_2\text{O}_3\text{:Si}$  on commercial FTO.

The XPS measurements were carried out immediately after the PLD growth using a Kratos Axis Supra DLD spectrometer with an Al  $K\alpha$  source ( $\lambda\nu = 1486.6 \text{ eV}$ ) operating at 150 W without any *ex situ* cleaning process. The measured binding energies were referenced to the C1s binding energy of the carbon contamination (284.8 eV) and the step size was set to 0.1 eV for high-resolution XPS acquisition. The binding energy peaks were fitted by Voigt curves using a Shirley background subtraction [34] in the proximity of the peak, while the valence band maximum (VBM) was calculated by extrapolating the leading edge to zero signal. The crystal structure of the thick  $\text{Ga}_2\text{O}_3\text{:Si}$  and the FTO films was examined by a Bruker D8 Advance x-ray diffractometer with a Cu  $K\alpha$  source ( $\lambda = 1.5405 \text{ \AA}$ ). The optical transmittance of the films was characterized by a Shimadzu UV-3600 spectrophotometer. Ti (20 nm)/Au (80 nm) contacts were deposited on a by DC sputtering at 440 W, followed by a rapid thermal annealing (RTA) treatment at  $470^\circ\text{C}$  for 60 s in Ar atmosphere, performed in a JetFirst 200C system. The  $I$ – $V$  curve of the junction was measured by a Keithley 2400 system.

Figure 2 shows the XRD patterns of the 350 nm  $\text{Ga}_2\text{O}_3\text{:Si}$  film on the FTO/glass substrate and the FTO/glass substrate itself. These patterns are compared with selected powder peaks of the following JCPDS-ICDD cards: 41-1445 for  $\text{SnO}_2$

**Table 1.** Peak positions of the core levels and VBM used to calculate the band offset in the  $\text{Ga}_2\text{O}_3\text{:Si}/\text{FTO}$  junction.

Sample	Region	Binding energy (eV)
$\text{Ga}_2\text{O}_3\text{:Si}$	Ga $2p_{3/2}$ VBM	1117.78 3.42
FTO	Sn $3d_{5/2}$ VBM	486.35 3.19
$\text{Ga}_2\text{O}_3\text{:Si}/\text{FTO}$	Ga $2p_{3/2}$ Sn $3d_{5/2}$	1118.00 486.38

tetragonal-rutile and 43-1012 for  $\text{Ga}_2\text{O}_3$  monoclinic. The FTO/glass substrate contains (101), (110), (200), (211), and (220) planes. As a result, the grown  $\text{Ga}_2\text{O}_3\text{:Si}$  film is expected to follow some of those planes regardless of the growth or epitaxy techniques. The deposited  $\text{Ga}_2\text{O}_3\text{:Si}$  film presents a monoclinic structure ( $\beta$ ) with two main orientations, predominantly (110) with (400) at much lower intensity (inset of figure 2). These growth directions are consistent with the intensity of the (110) and (200) peaks of the FTO film, indicating that  $\text{Ga}_2\text{O}_3$  grew following mainly the (110) plane and marginally the (200) plane of the FTO. Due to the monoclinic crystal structure of  $\text{Ga}_2\text{O}_3$ , the film did not grow in the direction of any of the other three planes, i.e. (101), (211), and (220) of the FTO/glass substrate.

To facilitate the determination of the band offsets, the bandgaps ( $E_g$ ) of  $\text{Ga}_2\text{O}_3\text{:Si}$  and FTO were first deduced from transmission spectra. Since  $E_g$  of  $\text{Ga}_2\text{O}_3$  is larger than that of FTO, it is not possible to measure it on the FTO/glass substrate. Thus, another 350 nm  $\text{Ga}_2\text{O}_3\text{:Si}$  layer was grown under the same conditions as the  $\text{Ga}_2\text{O}_3$  (350 nm)/FTO/glass sample on an optically transparent *c*-sapphire substrate. Figure 3 shows the transmission measurement for both films using the air baseline while the inset displays the Tauc plot [35] ( $h\nu$  versus  $(\alpha h\nu)^{1/n}$ ) in which  $n = 1/2$  was used for direct allowed transitions. The calculated  $E_g$  are  $4.94 \pm 0.01 \text{ eV}$  and  $4.40 \pm 0.02 \text{ eV}$  for  $\text{Ga}_2\text{O}_3\text{:Si}$  and FTO, respectively. In the case of  $\text{Ga}_2\text{O}_3\text{:Si}$ , an increment of  $E_g$  compared to undoped  $\text{Ga}_2\text{O}_3$  ( $E_g = 4.7\text{--}4.9 \text{ eV}$ ) [9, 10] has been observed concomitantly with the increase of Si content in the film [36]. The  $E_g$  of FTO is higher than some reported values ( $\sim 4.10 \text{ eV}$ ) [37, 38], but it agrees well with the transmission spectra from NANOCS which supplied the FTO substrates for this study [39].



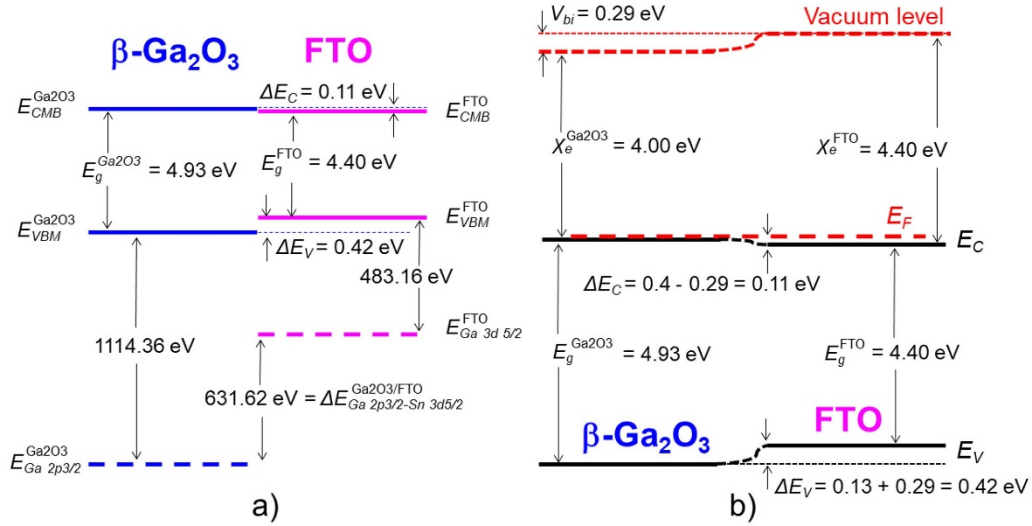


**Figure 5.** (a) Band alignment diagram for the Ga<sub>2</sub>O<sub>3</sub>/FTO heterojunction obtained by XPS and (b) the band diagram schematic with the band bending in the junction.

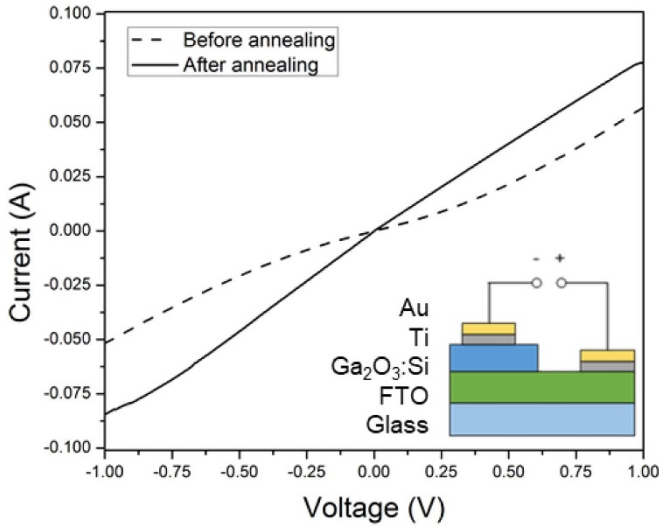


**Figure 6.** *I*–*V* curves of the Ga<sub>2</sub>O<sub>3</sub>:Si/FTO junction before and after the annealing process for the Ti/Au contacts. The inset shows the cross-sectional schematic.

To determine the band offsets at the heterojunction interface, Kraut's method [40] was utilized to analyze the XPS spectra of the three samples shown in figure 1. First, the core level binding energies and the VBM of the FTO and the 350 nm Ga<sub>2</sub>O<sub>3</sub>:Si layer were determined. The 3 nm Ga<sub>2</sub>O<sub>3</sub>:Si on FTO was measured for the binding energy difference between the two reference core levels at the interface. In all the peak fittings, the Shirley background and Voigt curves were employed. Figure 4 shows the XPS results. The selected core levels are Ga 2p<sub>3/2</sub> and Sn 3d<sub>5/2</sub> since these are the most intense peaks observed in the XPS survey spectra. The calculation of the VBM for both the Ga<sub>2</sub>O<sub>3</sub>:Si/FTO and FTO is shown in the insets of figures 4(a) and (b), respectively. One Voigt curve allowed the proper fitting of the Ga 2p<sub>3/2</sub> binding energy of both the thick as well as the thin Ga<sub>2</sub>O<sub>3</sub>:Si film on FTO

(figures 4(a) and (c)). On the other hand, the Sn 3d<sub>5/2</sub> peak is not symmetric due to the contribution of Sn<sup>4+</sup> and Sn<sup>2+</sup> (figures 4(b) and (c)) [41, 42]. Table 1 summarizes the core levels and VBM values of the samples.

Equations (1) and (2) are used to calculate the VBO and the CBO, respectively [11]. The sequence of the terms in parenthesis in equation (1) corresponds to the XPS results in figures 4(a)–(c). In order to calculate the CBO (equation (2)), the difference between the *E<sub>g</sub>* of Ga<sub>2</sub>O<sub>3</sub>:Si and FTO films was used:

$$\Delta E_V = (E_{\text{Ga2p}}^{\text{Ga}_2\text{O}_3} - E_{\text{VBM}}^{\text{Ga}_2\text{O}_3}) - (E_{\text{Sn3d}}^{\text{FTO}} - E_{\text{VBM}}^{\text{FTO}}) - (E_{\text{Ga2p}}^{\text{Ga}_2\text{O}_3} - E_{\text{Sn3d}}^{\text{FTO}}), \quad (1)$$

$$\Delta E_C = (E_g^{\text{Ga}_2\text{O}_3} - E_g^{\text{FTO}}) - \Delta E_V. \quad (2)$$

The diagram in figure 5(a) shows the band alignment diagram of the heterojunction. It shows that the Ga<sub>2</sub>O<sub>3</sub>:Si/FTO junction has a straddling-gap (type-I) alignment, with VBO ΔE<sub>V</sub> of 0.42 eV and CBO ΔE<sub>C</sub> of 0.11 eV. Since the ΔE<sub>C</sub> is small, this alignment is desirable for electron transport across the heterointerface. Previously, a type-I junction was reported for Ga<sub>2</sub>O<sub>3</sub> deposited by PLD on the (111) Si substrate with ΔE<sub>C</sub> as low as 0.2 eV [43]. In another study, the band offset of ITO/Ga<sub>2</sub>O<sub>3</sub> was ΔE<sub>C</sub> = 0.32 eV and a type-I junction [23]. Our results show twice and three times lower ΔE<sub>C</sub> than these two studies, respectively, which favors electron transport. There might be strain in the Ga<sub>2</sub>O<sub>3</sub> layer due to lattice mismatch. However, previous works have shown that the impact of strain on CBO and VBO is nearly negligible by comparing the unstrained and strained heterojunctions [44, 45].

Furthermore, the band bending for the Ga<sub>2</sub>O<sub>3</sub>:Si/FTO heterojunction is shown in figure 5(b), aligning the Fermi level of both materials. The effective density of states function in the conduction band for both materials was calculated considering


an effective electron mass ( $m_n^*$ ) of  $0.28m_o$  corresponding to  $\text{SnO}_2$  and  $\text{Ga}_2\text{O}_3$  [46, 47]. According to our Hall effect measurements at room temperature, the concentrations of electrons were  $9.1 \times 10^{20}$  and  $1.0 \times 10^{19} \text{ cm}^{-3}$  for FTO and  $\text{Ga}_2\text{O}_3\text{:Si}$  films, respectively. This measurement was performed using an Ecopia HMS-3000 Hall system with a 1 T magnet and following the van der Pauw method. Hence, the Fermi levels for the materials are located above the conduction band (0.14 eV for FTO and 0.03 eV for  $\text{Ga}_2\text{O}_3$ ). Considering the calculated Fermi levels and the reported electron affinities ( $\chi_e$ ) for  $\text{Ga}_2\text{O}_3$  (4.0 eV) and FTO (4.4 eV) [48, 49], a built-in potential ( $V_{bi}$ ) of 0.29 eV was obtained. A type-I junction is still observed with the same  $\Delta E_V$  and  $\Delta E_C$  compared to the band alignment study due to band bending. It is important to note that this treatment does not consider interface states. To investigate the electrical properties of the  $\text{Ga}_2\text{O}_3\text{:Si}/\text{FTO}$  and FTO/metal heterojunctions, we performed  $I$ - $V$  measurement at room temperature. Two sets of metallic masks were used, first to deposit the  $\text{Ga}_2\text{O}_3\text{:Si}$  thin film on the FTO/glass substrate and second to deposit two sets of  $1 \times 10 \text{ mm}^2$  Ti (20 nm)/Au (80 nm) contacts on the  $\text{Ga}_2\text{O}_3\text{:Si}$  thin film. The  $I$ - $V$  curve and the schematic are presented in figure 6. The  $I$ - $V$  curve was measured before and after RTA of the complete measured heterostructure at  $470^\circ\text{C}$  in Ar atmosphere to improve the quality of the Ti/Au contacts. After annealing, the resistance decreased significantly from approximately 27 to  $12 \Omega$  while the ohmic behavior was improved in the  $\pm 1 \text{ V}$ , indicating that FTO can be an encouraging current spreading layer for  $\text{Ga}_2\text{O}_3$ .

In summary, we reported on the formation and characterization of the  $\text{Ga}_2\text{O}_3\text{:Si}/\text{FTO}$  heterojunction. In particular, we have performed high-resolution XPS measurements to determine that the  $\text{Ga}_2\text{O}_3\text{:Si}/\text{FTO}$  heterojunction has a straddling-gap (type-I) alignment with  $\Delta E_V$  of 0.42 eV and  $\Delta E_C$  of 0.11 eV. The junction exhibits a pseudo-ohmic behavior with Ti/Au contacts after annealing. The small  $\Delta E_C$  and the non-rectifying behavior of the junction, as well as the large  $E_g$  of 4.40 eV and reported thermal stability at high temperature [22–24], make FTO a promising candidate for use as a current spreading layer in  $\text{Ga}_2\text{O}_3$ -based high temperature and short wavelength devices.

## Acknowledgments

The authors would like to acknowledge the support of KAUST Baseline BAS/1/1664-01-01, KAUST Competitive Research Grant URF/1/3437-01-01 and URF/1/3771-01-01, and GCC Research Council REP/1/3189-01-01.

## ORCID iDs

Carlos G Torres-Castanedo  <https://orcid.org/0000-0002-4505-7970>

Xiaohang Li  <https://orcid.org/0000-0002-4434-365X>

## References

- [1] Wong M H, Sasaki K, Kuramata A, Yamakoshi S and Higashiwaki M 2016 *IEEE Electron Device Lett.* **37** 212
- [2] Higashiwaki M, Sasaki K, Kuramata A, Masui T and Yamakoshi S 2012 *Appl. Phys. Lett.* **100** 013504
- [3] Chabak K D et al 2016 *Appl. Phys. Lett.* **109** 213501
- [4] Higashiwaki M et al 2016 *Appl. Phys. Lett.* **108** 133503
- [5] Green A J et al 2016 *IEEE Electron. Device Lett.* **37** 902
- [6] Mastro M A, Kuramata A, Calkins J, Kim J, Ren F and Pearton S J 2017 *ECS J. Solid State Sci. Technol.* **6** 356
- [7] Yu F-P, Ou S-L and Wu D-S 2015 *Opt. Mater. Express* **5** 1240
- [8] Higashiwaki M, Sasaki K, Kuramata A, Masui T and Yamakoshi S 2014 *Phys. Status Solidi a* **211** 21
- [9] Guo D Y, Wu Z P, An Y H, Guo X C, Chu X L, Sun C L, Li L H, Li P G and Tang W H 2014 *Appl. Phys. Lett.* **105** 023507
- [10] Ogita M, Higo K, Nakanishi Y and Hatanaka Y 2001 *Appl. Surf. Sci.* **721** 175
- [11] Bartic M, Baban C-I, Suzuki H, Ogita M and Isaki M 2007 *J. Am. Ceram. Soc.* **90** 2879
- [12] Liu H, Avrutin V, Izyumskaya N, Özgür Ü and Morkoç H 2010 *Superlattices Microstruct.* **48** 458
- [13] Muhammed M M, Roldan M A, Yamashita Y, Sahonta S-L, Ajia I A, Iizuka K, Kuramata A, Humphreys C J and Roqan I S 2016 *Sci. Rep.* **6** 29747
- [14] Muhammed M M, Alwadai N, Lopatin S, Kuramata A and Roqan I S 2017 *ACS Appl. Mater. Interfaces* **9** 34057
- [15] Kyrtos A, Matsubara M and Bellotti E 2018 *Appl. Phys. Lett.* **112** 032108
- [16] Chikoidze E et al 2017 *Mater. Today Phys.* **3** 118
- [17] Yao Y, Davis R F and Porter L M 2017 *J. Electron. Mater.* **46** 2053
- [18] Higashiwaki M, Sasaki K, Murakami H, Kumagai Y, Koukita A, Kuramata A, Masui T and Yamakoshi S 2016 *Semicond. Sci. Technol.* **31** 034001
- [19] Orita M, Hiramatsu H, Ohta H, Hirano M and Hosono H 2002 *Thin Solid Films* **411** 134
- [20] Oshima T et al 2016 *Japan. J. Appl. Phys.* **55** 1202B7
- [21] Carey P H IV, Ren F, Hays D C, Gila B P, Pearton S J, Jang S and Kuramata A 2017 *Appl. Surf. Sci.* **422** 179
- [22] Minami T, Miyata T and Yamamoto T 1999 *J. Vac. Sci. Technol. A* **17** 1822
- [23] Choi W-J, Kwak D-J, Park C-S and Sung Y-M 2012 *J. Nanosci. Nanotechnol.* **12** 3394
- [24] Chen C M, Hsu T-C and Cherg S-J 2011 *J. Alloys Compd.* **509** 872
- [25] Kwak D-J, Moon B-H, Lee D-K, Park C-S and Sung Y-M 2011 *J. Electr. Eng. Technol.* **6** 684
- [26] Stepanov S I, Nikolaev V I, Bougrov V E and Romanov A E 2016 *Rev. Adv. Mater. Sci.* **44** 63
- [27] Minami T and Miyata T 2008 *Thin Solid Films* **517** 1474
- [28] Gogova D, Wagner G, Baldini M, Schmidbauer M, Irmischer K, Schewski R, Galazka Z, Albrecht M and Fornari R 2014 *J. Cryst. Growth* **401** 665
- [29] Sasaki K, Higashiwaki M, Kuramata A, Masui T and Yamakoshi S 2013 *J. Cryst. Growth* **378** 591
- [30] Murakami H et al 2015 *Appl. Phys. Express* **8** 015503
- [31] Leedy K D et al 2017 *Appl. Phys. Lett.* **111** 012103
- [32] Müller S, von Wenckstern H, Splith D, Schmidt F and Grundmann M 2014 *Phys. Status Solidi a* **211** 34
- [33] Zhang F, Saito K, Tanaka T, Nishio M and Guo Q 2015 *J. Mater. Sci. Mater. Electron* **26** 9624
- [34] Shirley D A 1972 *Phys. Rev.* **55** 4709
- [35] Tauc J, Grigorovici R and Vancu A 1966 *Phys. Status Solidi b* **15** 627

- [36] Takakura K, Koga D, Ohyama H, Rafi J M, Kayamoto Y, Shibuya M, Yamamoto H and Vanhellefont J 2009 *Physica B* **404** 4854
- [37] Stjerna B, Olsson E and Granqvist C G 1994 *J. Appl. Phys.* **76** 3797
- [38] Rakhshani A E, Makdisi Y and Ramazaniyan H A 1998 *J. Appl. Phys.* **83** 1049
- [39] NANOCS 2018 FTO coated glass slides  $25 \times 75 \times 2$  mm (<http://www.nanocs.net/FTO-glass-5ohm-20.htm>) (Accessed: 26 May 2018)
- [40] Kraut E A, Grant R W, Wladrop J R and Kowalczyk S P 1980 *Phys. Rev. Lett.* **44** 1620
- [41] Yang J K, Zhao H L and Zhang F C 2013 *Mater. Lett.* **90** 37
- [42] Li T, Zhang X, Ni J, Fang J, Zhang D, Sun J, Wei C, Xu S, Wang G and Zhao Y 2016 *Sol. Energy* **134** 375
- [43] Chen Z, Nishihagi K, Wang X, Saito K, Tanaka T, Nishio M, Arita M and Guo Q 2016 *Appl. Phys. Lett.* **109** 102106
- [44] Van de Walle C G and Neugebauer J 1997 *Appl. Phys. Lett.* **70** 2577
- [45] Wei S and Zunger A 1996 *Appl. Phys. Lett.* **69** 2719
- [46] Button K J, Fonstad C G and Dreybrodt W 1971 *Phys. Rev. B* **4** 4539
- [47] Janowitz C, Scherer V, Mohamed M, Krapf A, Dwelk H, Manzke R, Galazka Z, Uecker R, Irmscher K and Fornari R 2011 *New J. Phys.* **13** 085014
- [48] Mohamed M, Irmscher K, Janowitz C, Galazka Z, Manzke R and Fornari R 2012 *Appl. Phys. Lett.* **101** 132106
- [49] Helander M G, Greiner Z, Wang Z B and Tang W M 2011 *J. Vac. Sci. Technol. A* **29** 011019